Resolving Length Scale Dependent Transient Disorder Through an Ultrafast Phase Transition

Supplementary Information

Jack Griffiths[1], Ana Flávia Suzana[1], Longlong Wu[1], Samuel D. Marks[2], Vincent Esposito[3], Sébastien Boutet[3], Paul G. Evans[2], J. F. Mitchell[4], Mark P. M. Dean[1], David A. Keen[5], Ian Robinson[1], Simon J. L. Billinge[1,6], Emil S. Bozin[1]

[1] *Condensed Matter Physics and Materials Science Division, Brookhaven National Laboratory, Upton, NY 11973, USA*
[2] *Department of Materials Science and Engineering, University of Wisconsin, Madison, WI 53706, USA*
[3] *SLAC National Accelerator Laboratory, 2575 Sand Hill Road, Menlo Park, California 94025, USA*
[4] *Materials Science Division, Argonne National Laboratory, Lemont, Illinois 60439, United States*
[5] *ISIS Neutron and Muon Source, STFC Rutherford Appleton Laboratory, Harwell Campus, Didcot, Oxfordshire OX11 0QX, United Kingdom*
[6] *Department of Applied Physics and Applied Mathematics, Columbia University, New York, New York 10027, USA*

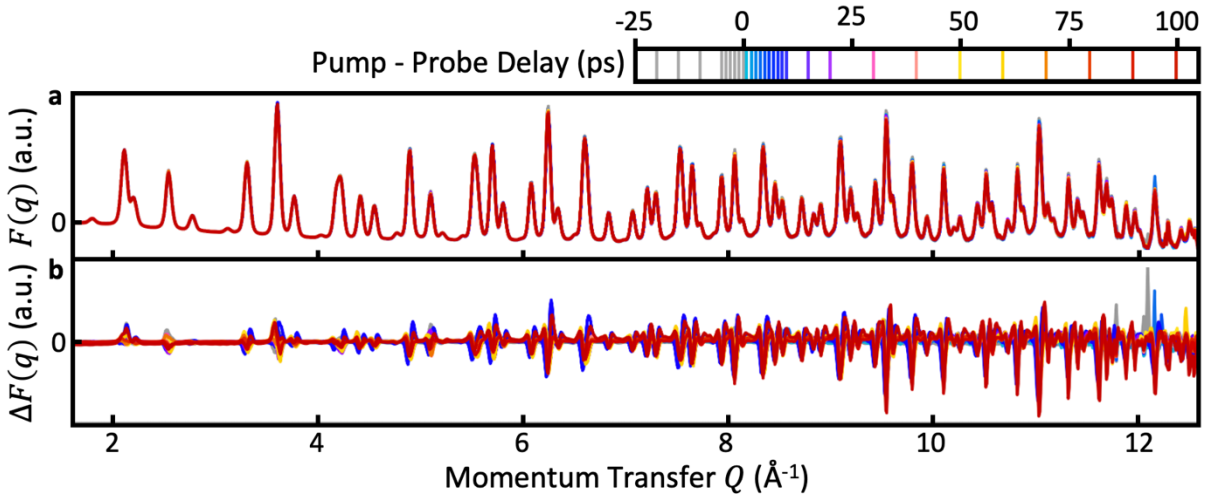

Supplementary Figure 1 | 300 K Pump Response. a) Reduced structure factor $F(Q)$ with varying pump-probe delay at 300 K using 27μJ of pump energy. All negative delay signals (unpumped measurements) are coloured grey. b) $\Delta F(Q)$ subtracting the average of {-20,-15,-10} ps to emphasise differences due to laser pump. Only a mild heating response (seen most clearly by the drop in high Q peak intensities) is seen. Any peak shift due to lattice shifting is much smaller than the peak width.

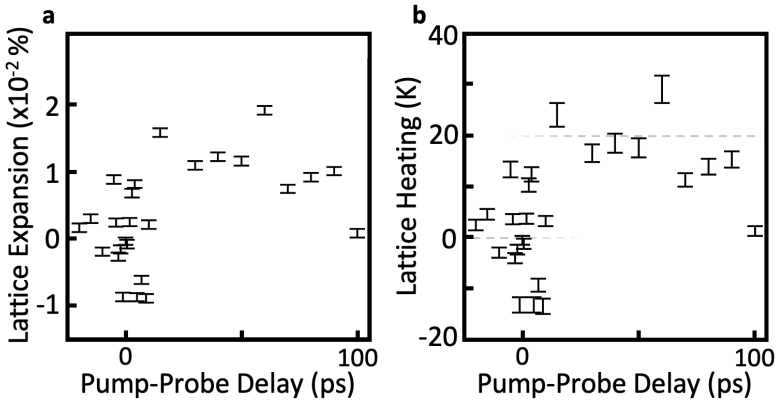

Supplementary Figure 2 | Room Temperature Lattice Heating. a) Thermal lattice expansion of the cubic metallic phase at 300 K under 27μJ of pump laser energy, extracted using the shift of Bragg diffraction peaks. Uncertainties are derived from maximum likelihood methods, but do not account for systematic effects while converting 2D diffraction images to 1D patterns that may increase uncertainty on these small shifts. b) Using APS synchrotron measurements of the same powder at equilibrium at 250 K and 300 K, this metallic phase is calculated to have a linear thermal expansion coefficient of (6.7 $\pm$ 0.6) x 10^{-6} K^{-1}. This converts the lattice expansion into approximately 20 K of laser heating. Note that the heating onset is delayed by approximately 10 ps in accordance with the two-temperature model of lattice heating. During the 150 K pump-probe experiments, 41 μJ of pump energy was used. This would have led to approximately 30 K of lattice heating, leaving the sample still approximately 50 K below the thermal transition temperature.

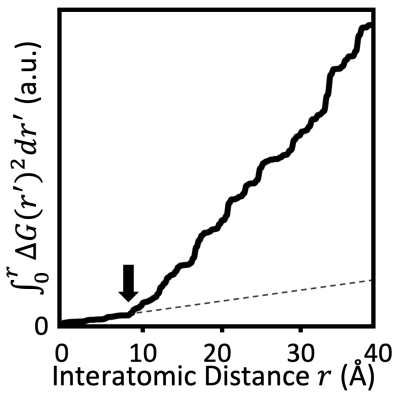

Supplementary Figure 3 | PDF Length Scale Ranges. Cumulative integral of 150 K $\Delta G(r)$ at 100 ps (Fig. 2d). This function is approximately piece-wise linear with an abrupt change in gradient at 9 Å (arrow) encoding a similarly abrupt increase in the magnitude of $\Delta G(r)$ past this distance. Dashed line is a guide to the eye continuing the low r line. If $\Delta G(r)$ was dominated by peak shifting due to lattice heating, this cumulative integral would approximate a smooth parabola rather than two linear segments.

Supplementary Note 1: Calculating Difference PDFs from Dimer Breaking

To calculate the difference PDF $\Delta G(r)$ over a wider *r*-range from breaking a single Ir-dimer, a large box model of low temperature CIS was formed from a 12 x 12 x 12 supercell of the $P\bar{1}$ unit cell described in the literature[1]. This model contains 27648 Ir atoms. A single pair of dimerized Ir, at an Ir^{4+}[1] and a neighboring Ir^{4+}[4] position (using the literature notation provided in the cited reference) were moved apart by 0.4 Å along the [$1\bar{1}0$] axis. Each atom was moved an equal distance from their center point. PDFs were calculated for both the unperturbed and altered structures and from these the difference PDF, $\Delta G(r)$ = $G(r)$ [altered] − $G(r)$ [unperturbed]. This $\Delta G(r)$ consists of a series of delta functions which are positive or negative depending on whether the altered structure has added or removed correlations at a given distance, respectively. These delta functions were then broadened by convoluting $\Delta G(r)$ with a Gaussian function with a width chosen to mimic the resolution of the experimental data. The same procedure was used to calculate $\Delta G(r)$ for a model where the Ir^{4+} ions in *every* dimer were moved apart (both the Ir^{4+}[1] − Ir^{4+}[4] and Ir^{4+}[2] − Ir^{4+}[3] dimers) to completely remove the dimerization within the $P\bar{1}$ structure. The two $\Delta G(r)$ were then scaled such that the intensities of the strong $\Delta G(r)$ peaks below *r* ~ 9 Å were approximately the same as those of the experimental $\Delta G(r)$ at short times. Scale factors of 4320 and 0.55 were required for the single dimer and all dimer breaking models, respectively. The correlations from the single dimer model become very small at longer distances; this converts to a calculated $\Delta G(r)$ containing significant noise at high-r because these correlations are multiplied by r when forming $\Delta G(r)$. These two calculated $\Delta G(r)$ are shown in Figure 2e where they are compared with an averaged experimental $\Delta G(r)$ which is the PDF data taken at 4, 5 and 6 ps minus data recorded at -20, -15 and -10 ps.

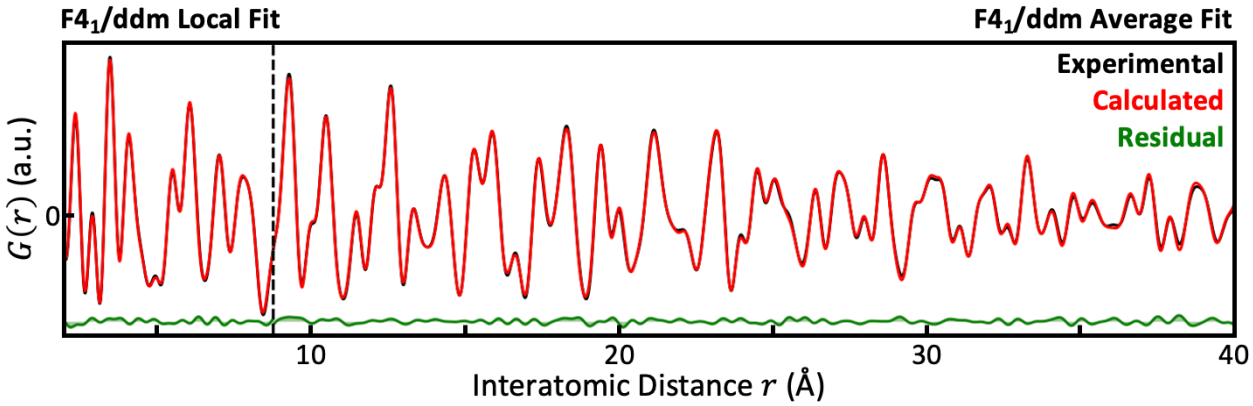

Supplementary Figure 4 | Example Pumped PDF Modelled. Experimental (black) and calculated (red) PDFs for 150 K pumped CIS at 100 ps pump-probe delay using the F4$_1$/ddm crystal group. Independent models are applied on the local and average ranges, separated by the vertical dashed line.

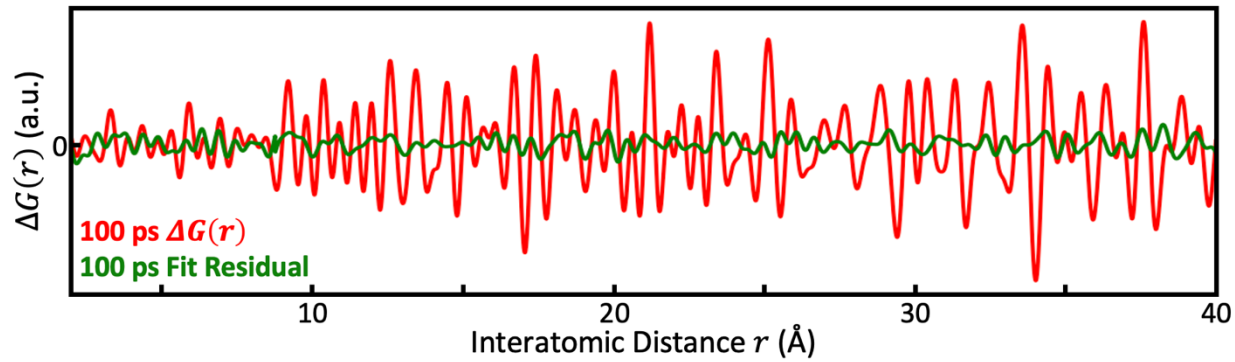

Supplementary Figure 5 | 100ps $\Delta G(r)$ v. Fit residual. $\Delta G(r)$ for the 150 K 100 ps pump probe delay measurement (red) as shown in Figure 2d. For comparison, the fit residual of this PDF is also shown (green) when using the F4$_1$/ddm crystal group, as shown in Supplementary Figure 3. The fit residual is significantly smaller in magnitude than the effect of the pump laser.

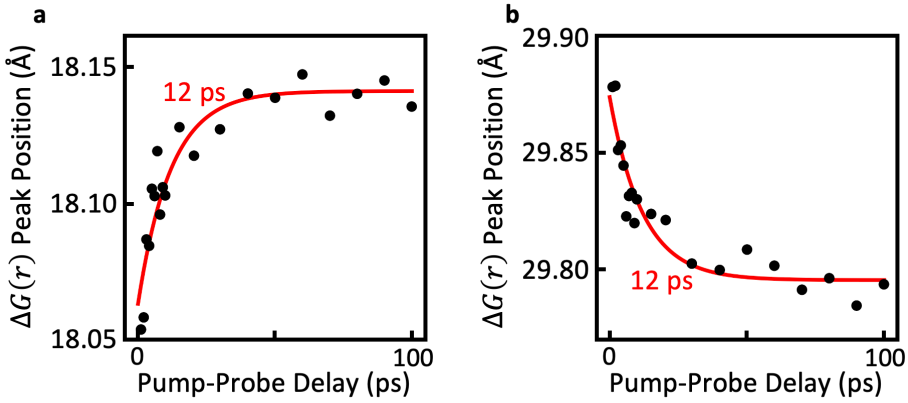

Supplementary Figure 6 | $\Delta G(r)$ Peak Shifting. Some peaks in $\Delta G(r)$ (Fig. 2d) shift subtly with pump-probe delay. This does not indicate simple lattice expansion, as not all peaks shift and those that do can shift to a) higher or b) lower interatomic distances. This shifting matches well to the 12 ps timescale extracted from structural modelling (red lines).

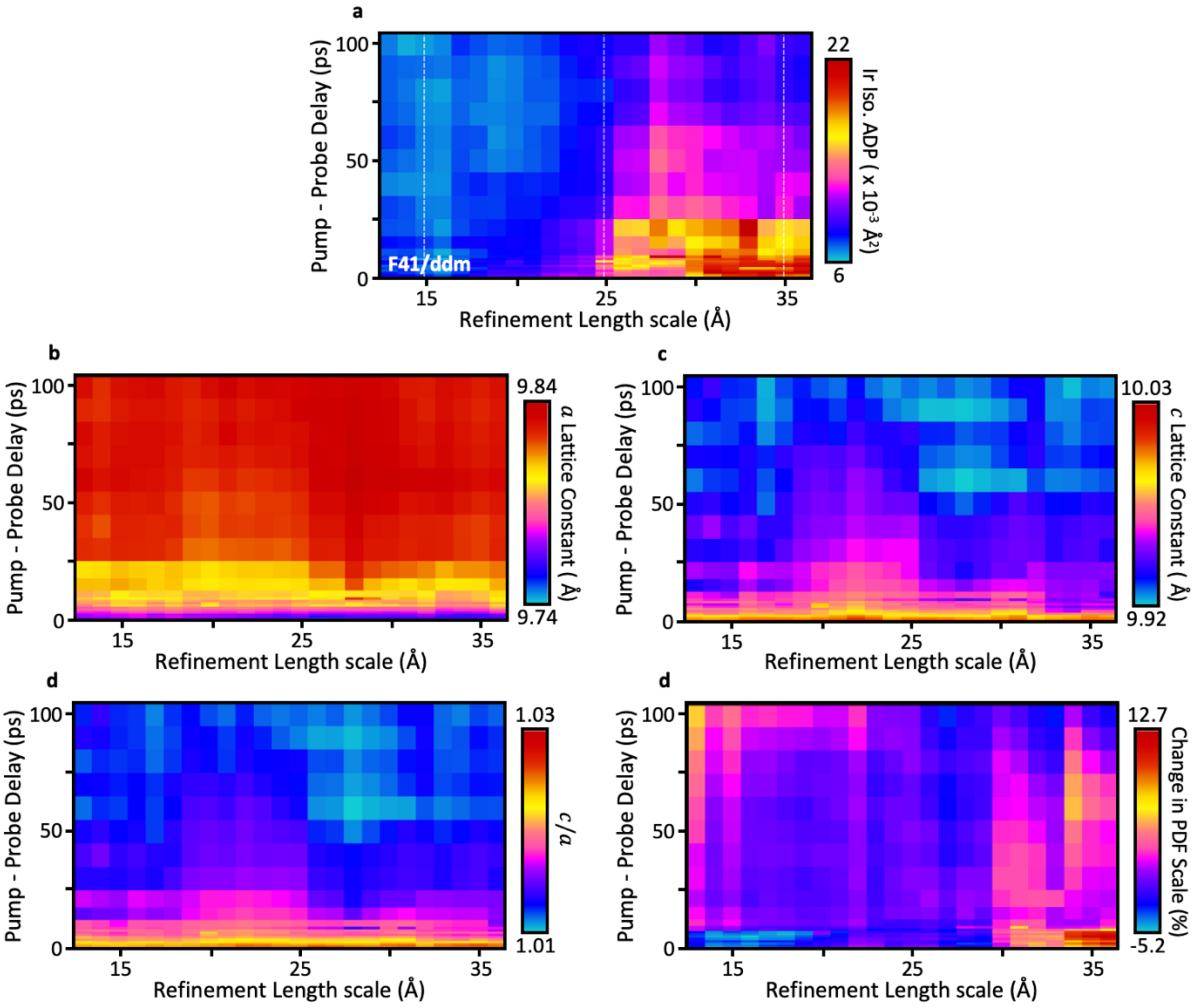

Supplementary Figure 7 | PDF Sliding Window Refinements. $F4_1/ddm$ model refined over a sliding widow of width 8.2 Å. Refinement Length Scale indicates the center of the refinement window. a) The isotropic Ir ADP as shown in Figure 4a. The ensure this is not an artifact of correlated refinement parameters, the a) a lattice constant, b) c lattice constant and c) a/c ratio do not display changes correlated with the Ir ADPs. (Fig. 4a). d) The scale factor used to match the experimental and modelled PDFs, normalized by the mean average for each pump-probe delay, also does not show the same length scale dependance.

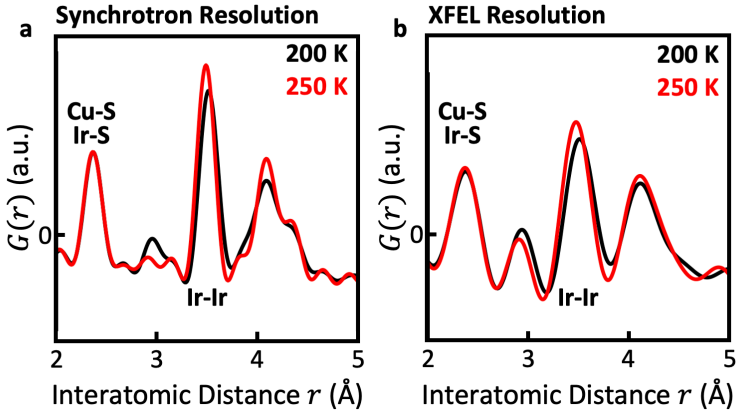

Supplementary Figure 8 | Equilibrium Synchrotron Measurements. a) Unpumped CIS PDF measured at the APS synchrotron above and below the transition temperature using a high maximum Q of 23 Å^{-1}. The dimerization signature around the Ir-Ir peak is clear while the first peak (Cu-S and Ir-S) is left insignificantly changed. b) These observations hold when artificially reducing the Q range of this same data to match the XFEL experiment in this work, lowering the PDF resolution.

1. Radaelli, P. G. *et al.* Formation of isomorphic Ir3+ and Ir4+ octamers and spin dimerization in the spinel $CuIr_2S_4$. *Nature* **416**, 155–158 (2002).